Electronic Supplementary Information

The catalytic behaviour in aqueous-phase hydrogenation over a renewable Ni catalyst derived from perovskite-type oxide

Chun Chen,[a] Ruoyu Fan,[a] Wanbing Gong,[a] Haimin Zhang,[a] Guozhong Wang[a] and Huijun Zhao*[ab]

[a] Key Laboratory of Materials Physics, Centre for Environmental and Energy Nanomaterials, Anhui Key Laboratory of Nanomaterials and Nanotechnology, CAS Centre for Excellence in Nanoscience, Institute of Solid State Physics, Chinese Academy of Sciences, Hefei 230031, P. R. China

[b] Centre for Clean Environment and Energy, Gold Coast Campus, Griffith University, Queensland 4222, Australia

Address correspondence to h.zhao@griffith.edu.au; gzhwang@issp.ac.cn

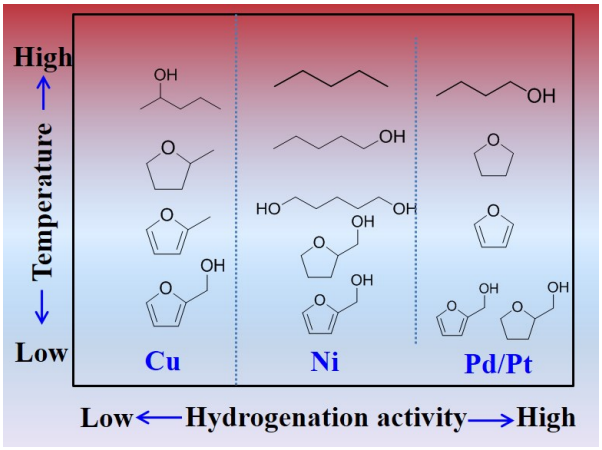

Fig. S1 The comparison of Ni catalyst with Cu and Pd/Pt catalysts in hydrogenation of furfural

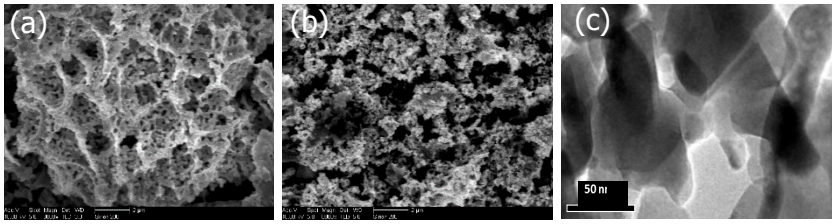

Fig. S2 The morphology of $LaNiO_3$ precursor and Ni-LN650.

(a) SEM image of $LaNiO_3$, (b) SEM image of Ni-LN650, (c) TEM image of Ni-LN650.

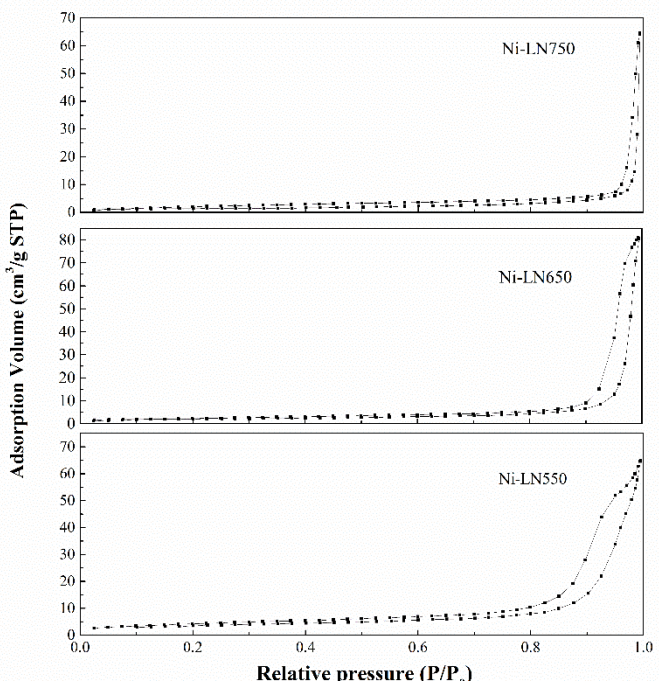

Fig. S3 Adsorption and desorption isotherm curves of Ni-LN550, Ni-LN650 and Ni-LN750 catalysts.

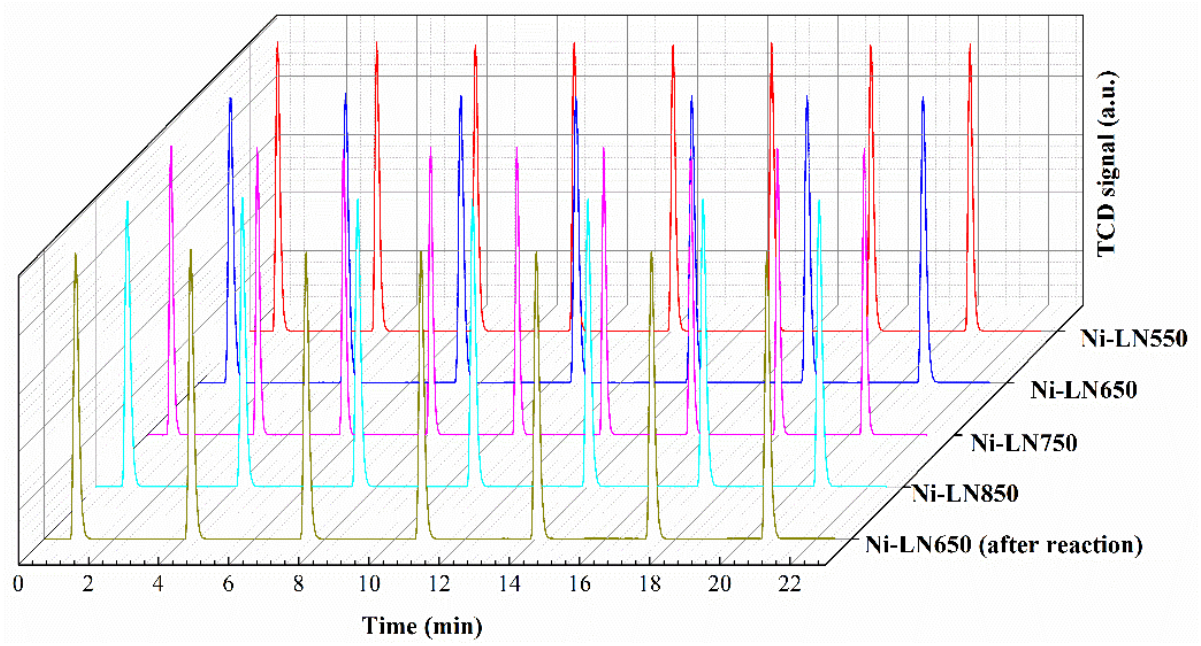

Fig. S4 the CO pulse chemisorption for Ni-LN550, Ni-LN650, Ni-LN750, Ni-LN850 and Ni-LN650 (after reaction)

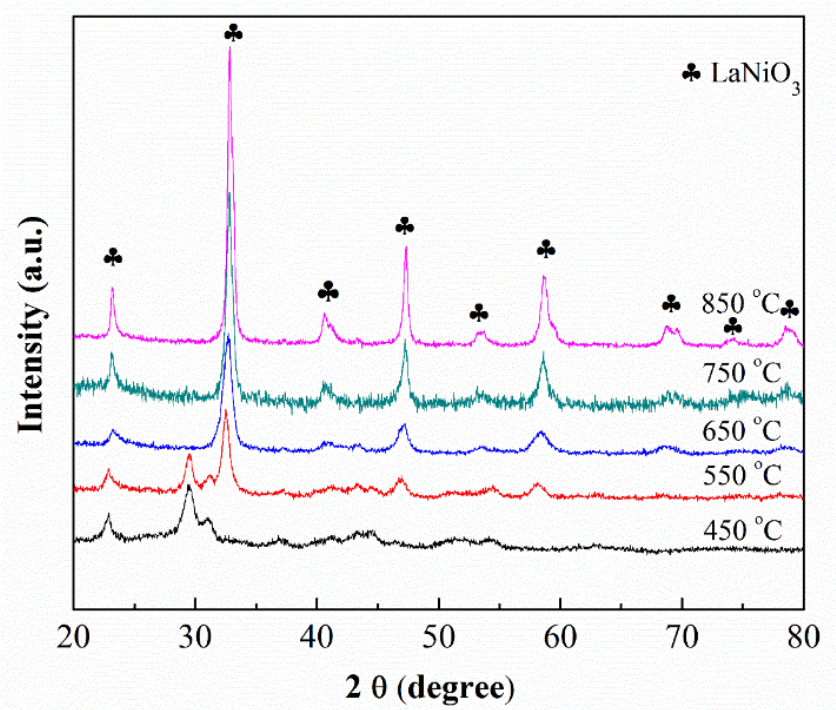

Fig. S5 The XRD patterns of $LaNiO_3$ precursor derived at different calcination temperatures.

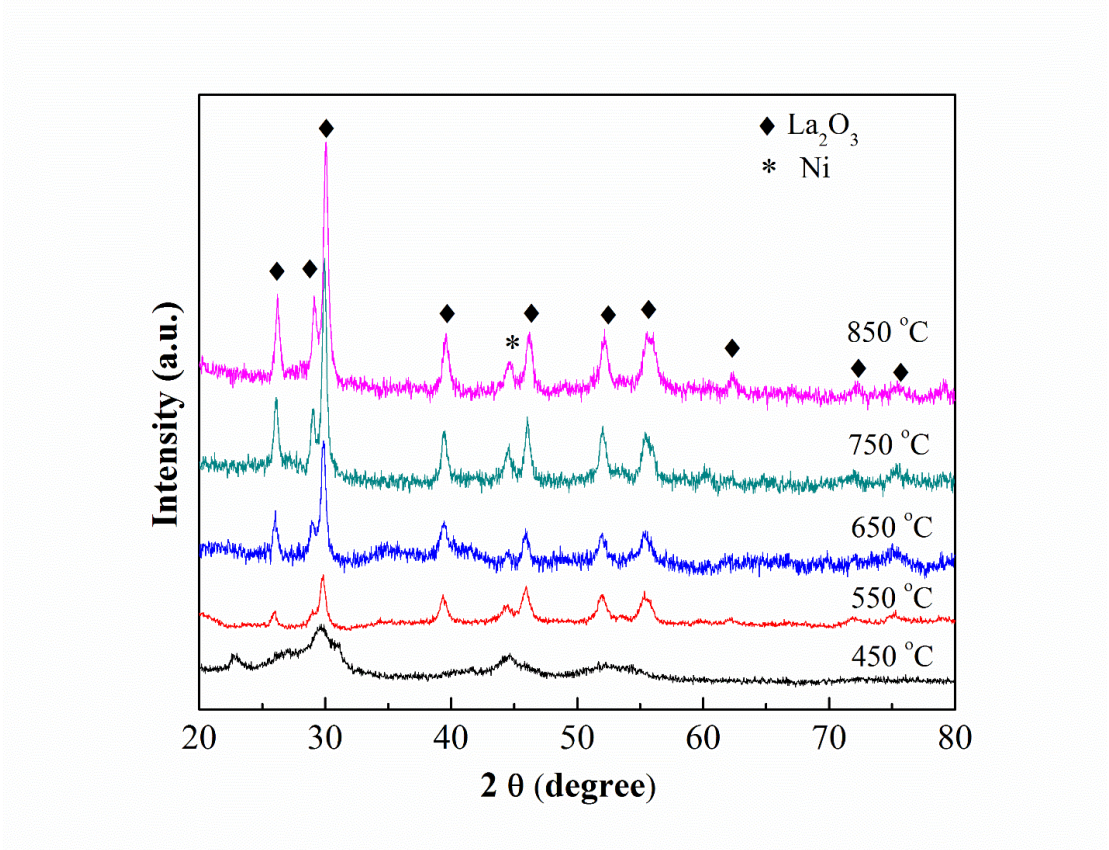

Fig. S6 The XRD patterns of Ni catalysts derived from the $LaNiO_3$ precursors calcining at different temperatures.

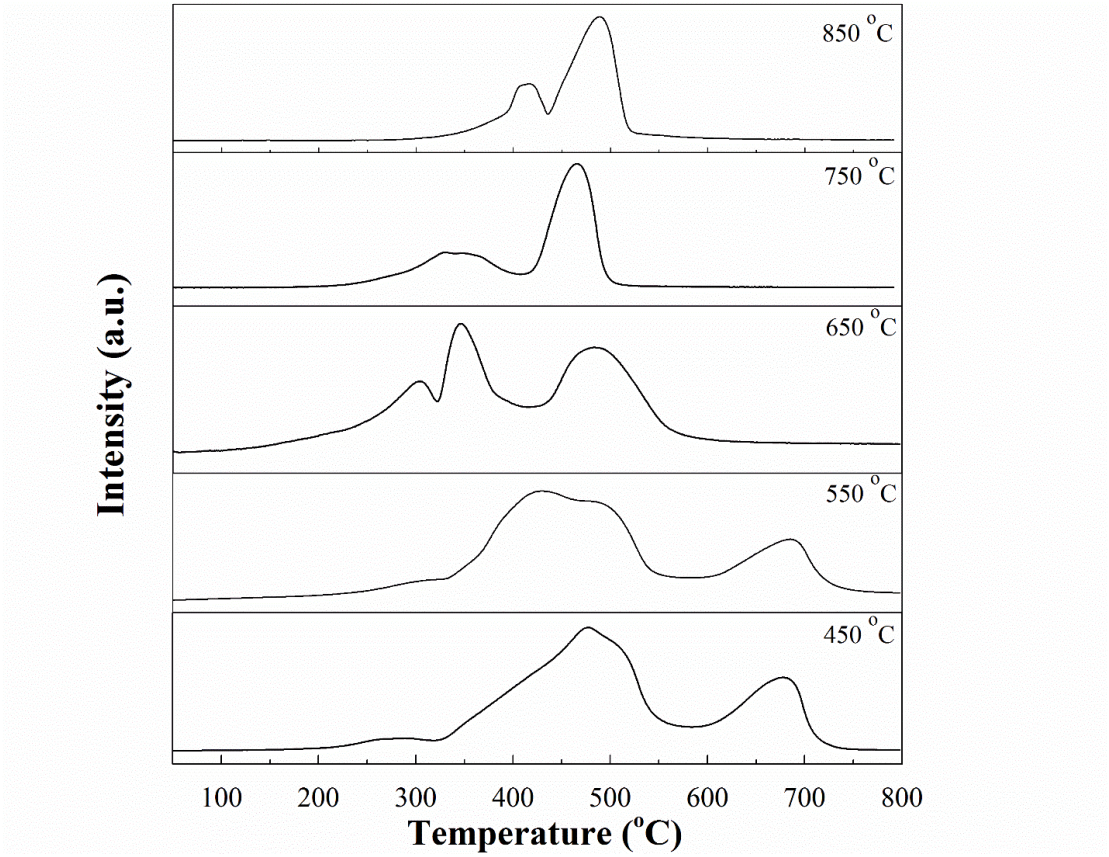

Fig. S7 The H_2-TPR profiles of $LaNiO_3$ precursor derived at different calcination temperatures.

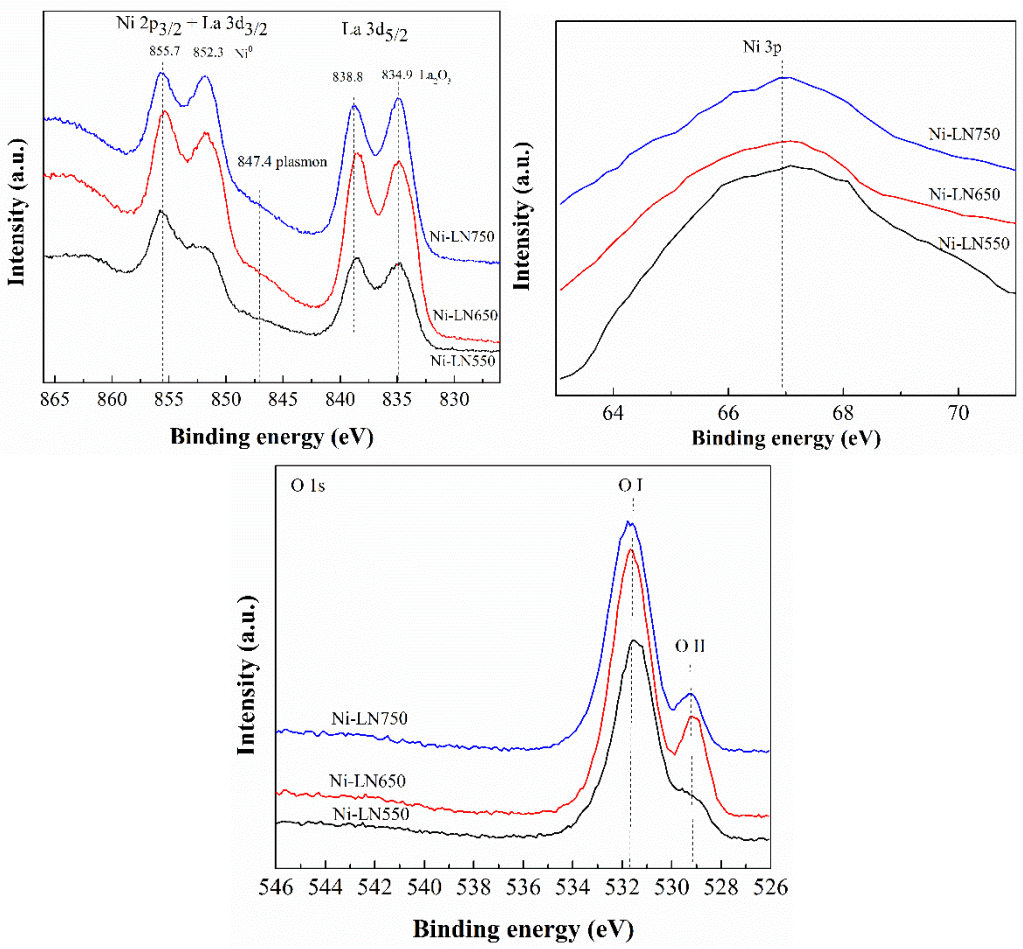

Fig. S8 The XPS spectra of La 3d+ Ni 2p, Ni3p and O 1s for the Ni-LN550, Ni-LN650 and Ni-LN750 catalysts.

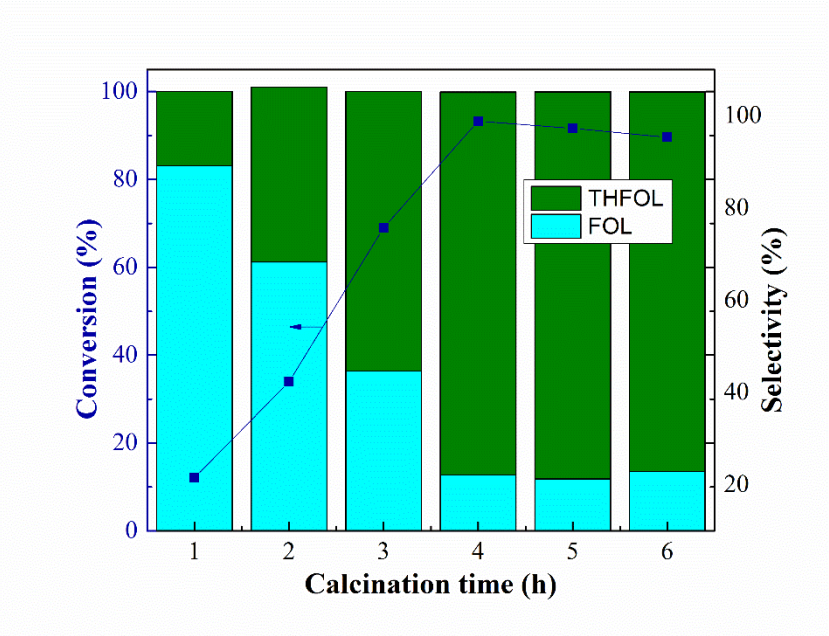

Fig. S9 The influence of calcination time on furfural conversion and product selectivity in aqueous-phase hydrogenation of furfural at 120 ^{o}C and 1 MPa H_2. Other conditions: 1.0 mmol furfural, 30 mg catalyst, 10 mL DI water, stirring speed 800 rpm.

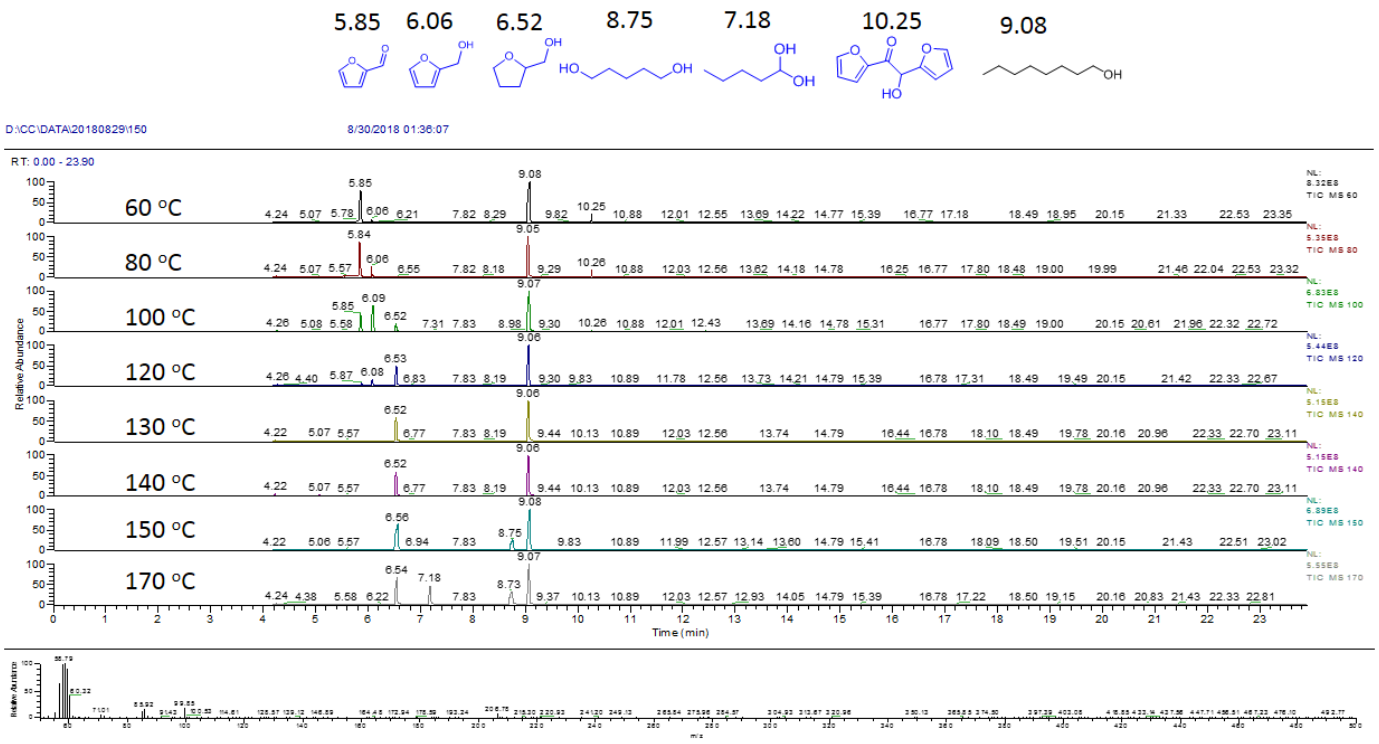

Fig. S10 The GC-MS spectrogram of liquid products obtained at different reaction temperature.

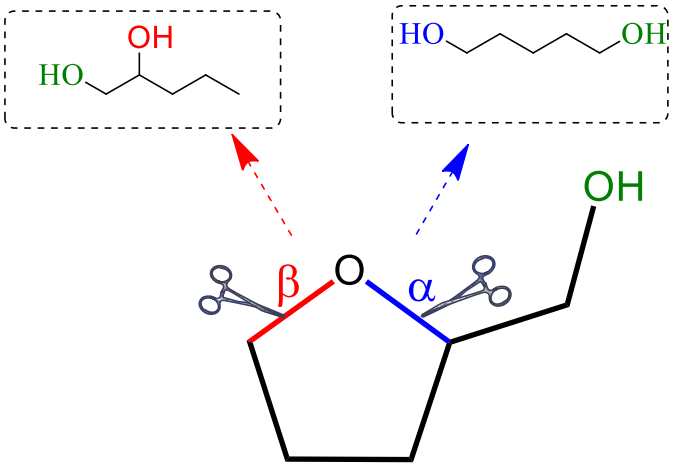

Fig. S11 The scission of THFOL at α and β positions.

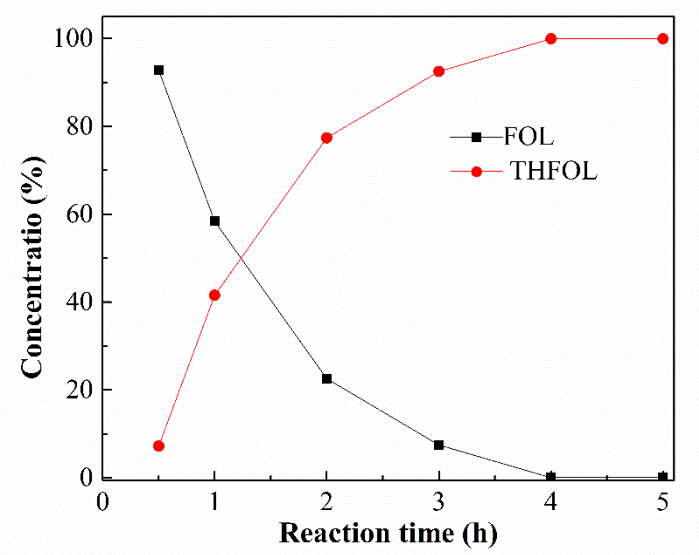

Fig. S12 The concentration of FOL and THFOL in the liquid product by using FOL as reactant.

Reaction condition: 120 °C, 1 MPa H2, 1 mmol FOL, 30 mg Ni-LN650, 10 mL DI water, stirring speed 800 rpm.

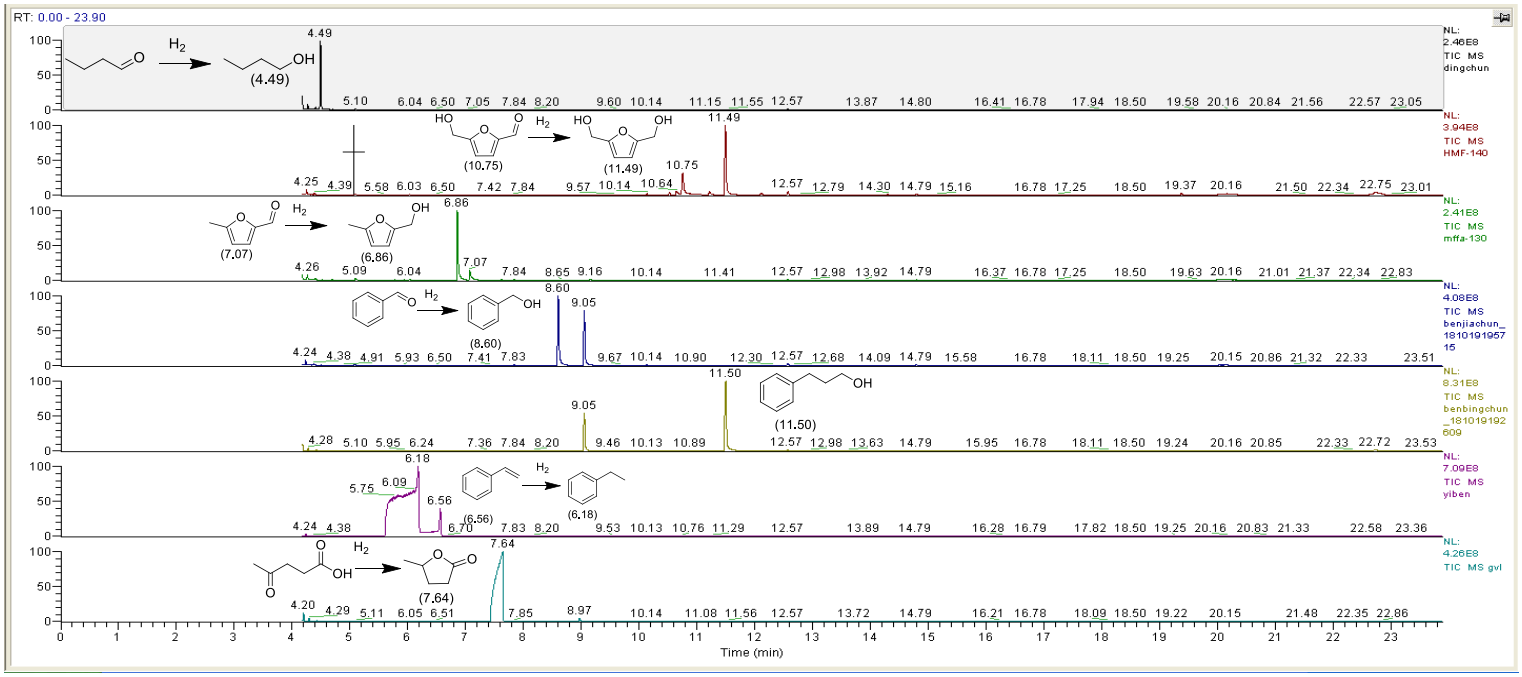

Fig. S13 The GC-MS spectrogram for aqueous-phase hydrogenation of aldehydes, alkene and carboxylic acid over Ni-LN650 catalyst

Table S1 The Ni dispersion and other properties of Ni-based catalysts

Catalyst	Ni content (%)[a]	Ni dispersion (%)[b]	Metallic surface area (m^2/g_{Ni}) [b]	Active Ni diameter (nm) [b]
Ni-LN550	25.7	10.8	71.8	9.4
Ni-LN650	26.2	30.8	205.2	3.3
Ni-LN750	25.6	25.2	167.9	4.1
Ni-LN850	26.4	24.1	160.6	4.3
Ni-LN650 (after reaction)	25.3	26.5	177.3	3.8

[a]: determined by ICP;

[b]: calculated from CO pulse chemisorption.

CO pulse chemisorption: 30 mg catalyst sample was loaded in U type quartz tube and installed in Micromeritics AutoChem II 2920 instrument. The sample was pretreated at 300 ^{o}C by a He gas for 1 h. After the sample was cooled to room temperature, the CO pulse chemisorption was tested until the pulse peak become stable (carrier gas: He; Pulse gas: CO).

Table S2 The comparison of Ni-LN650 with impregnated Ni/La2O3 and Raney Ni catalyst in aqueous-phase hydrogenation of furfural

Catalyst	Furfural conversion (%)	FOL selectivity (%)	THFOL selectivity (%)
Ni-LN650	98.8	12.7	87.2
Impregnated Ni/La_2O_3	84.3	25.4	74.5
Raney Ni (particle size $\leq$ 50μm, dispersed in water)	95.8	18.6	81.3

Reaction conditions: Ni-LN650 and Ni/La_2O_3 30 mg, Raney Ni 1 mL; 120 ^{o}C and 1 MPa H_2 for 3 h, 1mmol furfural, 10 mL DI water.